

The Biomechanical Properties of Meshed versus Perforated Acellular Dermal Matrices (ADMs)

Keith Sweitzer, MD*
 Katherine H. Carruthers, MD,
 MS†
 Lauren Blume, BS, CTBS‡
 Pankaj Tiwari, MD§
 Ergun Kocak, MD, MSS§

Background: Acellular dermal matrices (ADMs) are used for soft tissue augmentation across surgical specialties. Since allograft incorporation depends on direct opposition between the ADM and a vascular bed, seroma formation can be detrimental to incorporation. Since most ADM products are available in many meshed and perforated forms, there is a lack of consistency between manufacture designs. We set out to determine the fluid egress properties and increase in surface area resulting from common cut patterns.

Methods: Three ADM cut patterns were studied: 1 meshed and 2 perforated. We calculated the surface area of these modified ADM samples. Fluid was passed through each ADM, and time required for fluid passage was recorded. An ANOVA ($P < 0.05$) was used to determine if there was a significant difference in egress properties across the 3 patterns.

Results: Meshing in a 1:1 pattern resulted in a 97.50% increase in surface area compared with the uncut product. In comparison, only a 0.30% increase resulted from Perforation Pattern #1 and a 0.59% increase resulted from Perforation Pattern #2. There was a significant difference in egress properties across the three cut patterns ($P = 0.000$). The average egress time of Mesh Pattern #1 was 1.974 seconds. The average egress time of Perforation Pattern #2 was 6.504 seconds, and of Perforation Pattern #1 was 10.369 seconds.

Conclusions: Quantitative comparison revealed that meshing ADM significantly improves fluid egress and increases the surface area. Therefore, the use of meshed ADM tissue could improve the incorporation of ADM with the recipient, with improved patient outcomes. (*Plast Reconstr Surg Glob Open* 2021;9:e3454; doi: 10.1097/GOX.0000000000003454; Published online 11 March 2021.)

INTRODUCTION

Acellular dermal matrices (ADMs) are being used for soft tissue augmentation with increasing frequency across surgical specialties.^{1,2} These products are produced from human cadaveric donors and undergo a proprietary process of cleaning, rinsing, and decellularizing, which results in significant removal of cellular debris, including DNA, RNA, proteins, and antigens. The final product is a 3-dimensional, collagen-rich, biocompatible, non-cytotoxic matrix that retains its original biomechanical properties.³ The graft is then ready for implantation into the

recipient patient, where it is subsequently revascularized and the cell population is replaced as early as 8 weeks after placement.⁴

The increased use of ADMs has been particularly apparent in the setting of implant-based breast reconstruction, where matrices are used to supplement the thickness of the mastectomy skin flaps and ensure adequate soft tissue coverage of implants.^{5,6} However, long-term review of these devices has indicated that there is a strong correlation between seroma formation and the use of ADM.⁷⁻⁹ Because allograft integration and neovascularization is dependent on having direct opposition between the ADM and a vascular bed, the presence of seromas can inhibit the area of the graft that is in contact with the native tissue.¹⁰

To combat this challenge, most ADM products are available in a variety of meshed or perforated forms, which not only increases the surface area of the product but allows for active fluid egress, thus increasing the ability of the matrices to integrate into the surrounding native tissues.¹¹ Because of the lack of consistency between manufacture designs for meshing or perforation, we set out to determine the fluid egress properties and the increase

From the *Department of Surgery, Division of Plastic Surgery, University of Rochester, Rochester, N.Y.; †Department of Surgery, Division of Plastic Surgery, West Virginia University, Morgantown, W.Va.; ‡AlloSource, Centennial, Colo.; and §Midwest Breast and Aesthetic Surgery, Gahanna, Ohio.

Received for publication June 11, 2020; accepted December 22, 2020.

Copyright © 2021 The Authors. Published by Wolters Kluwer Health, Inc. on behalf of The American Society of Plastic Surgeons. This is an open-access article distributed under the terms of the [Creative Commons Attribution-Non Commercial-No Derivatives License 4.0 \(CCBY-NC-ND\)](https://creativecommons.org/licenses/by-nc-nd/4.0/), where it is permissible to download and share the work provided it is properly cited. The work cannot be changed in any way or used commercially without permission from the journal.

DOI: 10.1097/GOX.0000000000003454

Disclosure: The authors have no financial interest to declare in relation to the content of this article.

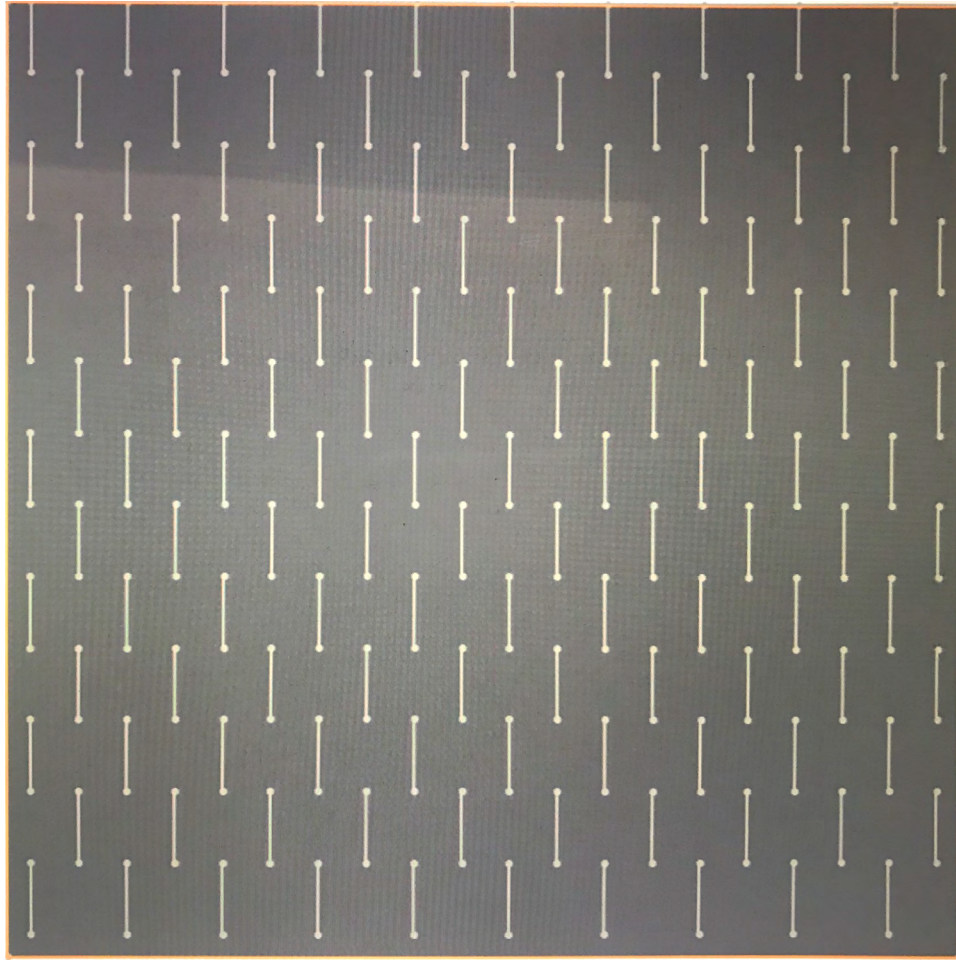


Fig. 1. Mesh pattern #1. Meshed cuts, each measuring 1.5 mm in length, are placed in a 1:1 distribution.

in surface area resulting from each of the common cut patterns.

METHODS

This study analyzed the fluid egress and surface area for 3 different commonly encountered commercially available ADM cut patterns: 1 meshed design and 2 distinct perforation designs. Mesh Pattern #1 was designed with 1:1 meshed cuts each measuring 1.5 mm in length (Fig. 1). Perforation Pattern #1 was designed with 3-mm diameter perforations at a density of 0.128 perforations per cm^2 (Fig. 2). Perforated Pattern #2 was designed with 3-mm diameter perforations at a density of 0.25 perforations per cm^2 (Fig. 3).

Six full-thickness ADM tissues from 3 different donors were processed (AlloMend, AlloSource, Centennial, Colo.). From each donor, 2 samples were prepared with Mesh Pattern #1, 2 with Perforation Pattern #1, and 2 with Perforation Pattern #2. Thus, the study utilized a total of 18 samples, with 6 of each cut pattern. A sample thickness of each sheet of product was measured to the nearest hundredth of a millimeter in 5 locations with a caliper

and recorded to account for a possible variation between donors and tissue source locations.

Determining Fluid Egress

A testing device was designed to measure the fluid egress properties of the 18 total tissue samples. Each ADM sample was placed between 2 pipe flanges with a valve below and clear pipe above (Fig. 4). The pipe was filled with fetal bovine serum (FBS). The valve was opened, allowing fluid to flow through the sample (Fig. 5). A camera recorded the amount of time (in seconds) required for the FBS to pass between 2 marked lines on the pipe (distance: 21.6 cm) (Fig. 5). Each sample was run in triplicate.

Average egress times, SDs, and 95% confidence intervals were calculated for each of the cut patterns. MiniTab 17 (MiniTab, LLC., State College, Penn.) was used to calculate a one-way ANOVA to determine if there was a significant difference in egress properties across the 3 patterns and a general linear model ANOVA was used to determine if variation in the tissue donor or graft thickness had a significant impact on the results. $P < 0.05$ was used to determine statistical significance. Specific mathematical equations are included below.

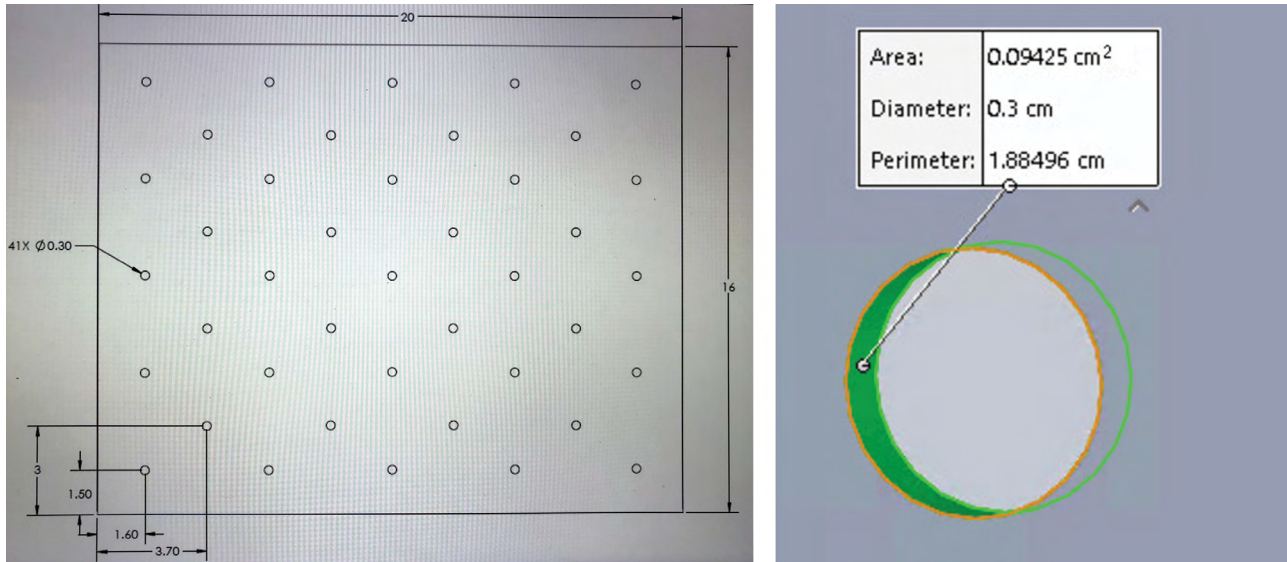


Fig. 2. Perforated pattern #1. Perforations are 3 mm in diameter at a density of 41 perforations per 320 cm² or approximately 0.128 perforations per cm². All dimensions are in centimeters.

Determining Surface Area

Meshing or perforating ADM tissue can change its surface area due to the additional area inside the pores or mesh. However, unlike meshing, perforation also removes a portion of surface area to create the holes. The surface area of these modified ADM samples is calculated based on the length, width, and thickness of the graft, and also must account for the mesh length or the perforation diameter and frequency. SolidWorks was used to visualize each of the 3 cut patterns.

The surface area of a perforated ADM graft is reduced when holes are stamped into the product, but simultaneously, the surface area is increased by the addition of new

walls inside the hole. Therefore, the surface area of a perforated graft can be calculated as follows:

$$\begin{aligned}
 \text{Surface Area}_{\text{perforated}} = & \\
 & (\text{original area}^*) + (\# \text{ holes}) + (\text{perimeter of each hole}) \\
 & \times (\text{graft thickness}) - (\# \text{ holes}) \\
 & \times (\text{crosssectional area of each hole})
 \end{aligned}$$

OR

$$\begin{aligned}
 \text{Surface Area}_{\text{perforated}} = & (\text{area of top graft}) + (\# \text{ holes}) \\
 & \times (\text{area of inside of hole})
 \end{aligned}$$

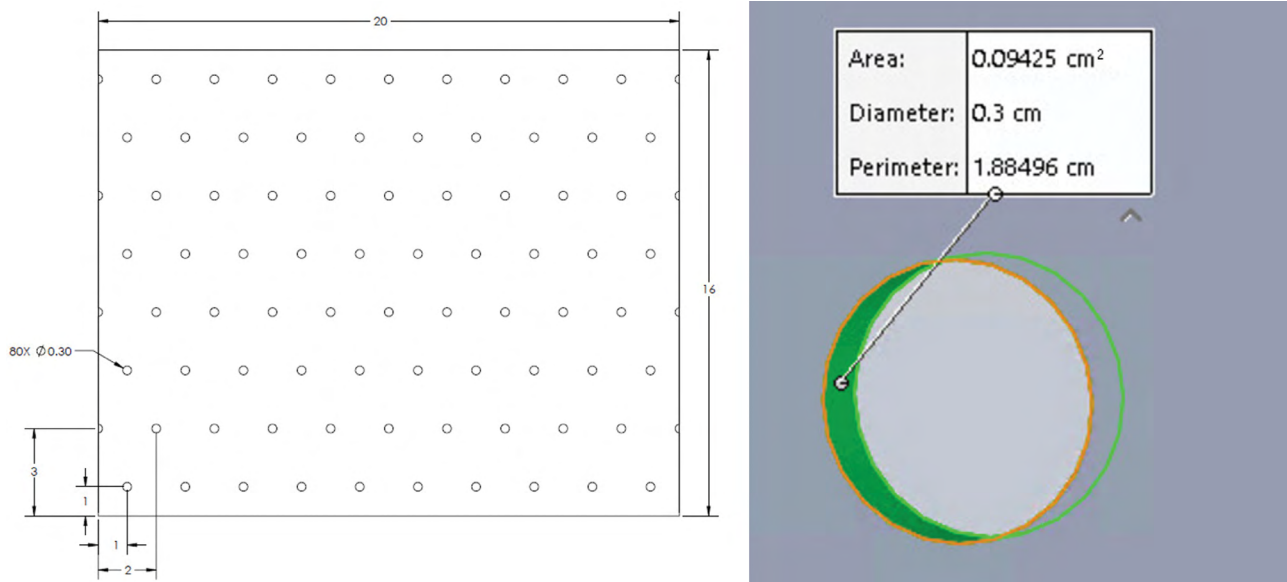


Fig. 3. Perforated pattern #2. Perforations are 3 mm in diameter at a density of 80 perforations per 320 cm² or approximately 0.25 perforations per cm². All dimensions are in centimeters.

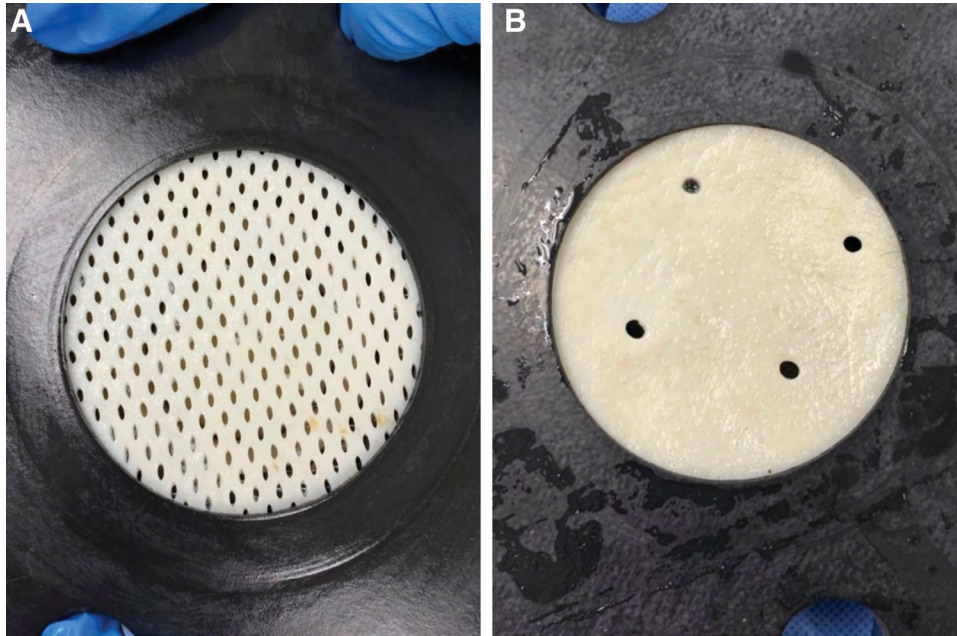


Fig. 4. Representative photographs of meshed (A) and perforated product (B) placed in the fluid egress testing device.

(*“Original Area” refers to the surface area (length × width) of the unperforated graft.). Unlike the perforating process, meshing does not remove any material from the graft. Instead, small lines are cut into the tissue and, as the graft is stretched, each line becomes a small pore. Thus, the surface area of a meshed graft is equal to the entire surface area of the top of the graft plus the area inside the pores. The total surface area of a meshed tissue is calculated as follows:

$$\text{Surface Area}_{\text{Meshed}} = (\text{original area}^*) + (\# \text{ mesh lines}) \times (\text{perimeter of mesh hole}) \times (\text{graft thickness})$$

The percent increase in surface area from either perforating or meshing is:

$$\text{Percent Increase in Surface Area}_{\text{Perforated or Meshed}} = \frac{(\text{modified surface area} - \text{original surface area})}{\text{original surface area}} \times 100$$

RESULTS

Analyzing Fluid Egress

There was a significant difference in egress properties across the three cut patterns ($P = 0.000$) (Fig. 6). The average egress time of Mesh Pattern #1 ADM was 1.974 seconds (SD 1.157 seconds). The average egress time of Perforation #2 pattern ADM was 6.504 seconds (SD 1.273 seconds) and of the Perforation Pattern #1 ADM was 10.369 seconds (SD 1.598 seconds) (Table 1). Note that the time required for the FBS to pass through the testing device is inversely

proportional to the volumetric flow rate through the graft (ie, a lower time indicates a higher volumetric flow rate).

$$\text{Volumetric Flow Rate} = \frac{\text{Volume}}{\text{Time}}$$

Neither donor ($P = 0.249$) nor graft thickness ($P = 0.914$) had a significant impact on the results. Thus, the meshed ADM tissue had an average volumetric flow rate of approximately 5.3 times that of the Perforated Pattern #1 tissue and approximately 3.3 times the flow rate of the Perforated Pattern #2 tissue.

Analyzing Surface Area

The surface area calculations for each type of cut pattern are noted below. The tissue thickness was assumed to be 1 mm for the purpose of this analysis.

Mesh Pattern

In a 16×20 cm graft, there are 10,400 mesh lines, each mesh line measuring 1.5 mm in length. The calculation for the surface area of a meshed tissue is as follows:

$$\begin{aligned} \text{Surface Area}_{\text{Mesh}} &= (\text{original area}) + (\# \text{ mesh lines}) \\ &\quad \times (\text{perimeter of mesh hole}) \times (\text{graft thickness}) \\ \text{Surface Area}_{\text{Mesh}} &= 320\text{cm}^2 + (10,400) (2 \times 1.5\text{mm}) (1\text{mm}) \end{aligned}$$

$$\begin{aligned} \text{Surface Area}_{\text{Mesh}} &= 320\text{cm}^2 + 312\text{cm}^2 = 632\text{cm}^2 \\ \text{Increase in Surface Area from Meshing} &= \frac{(632 - 320)}{320} \times 100 = 97.5\% \end{aligned}$$

Thus, meshing in a 1:1 pattern nearly doubles the surface area of the graft.

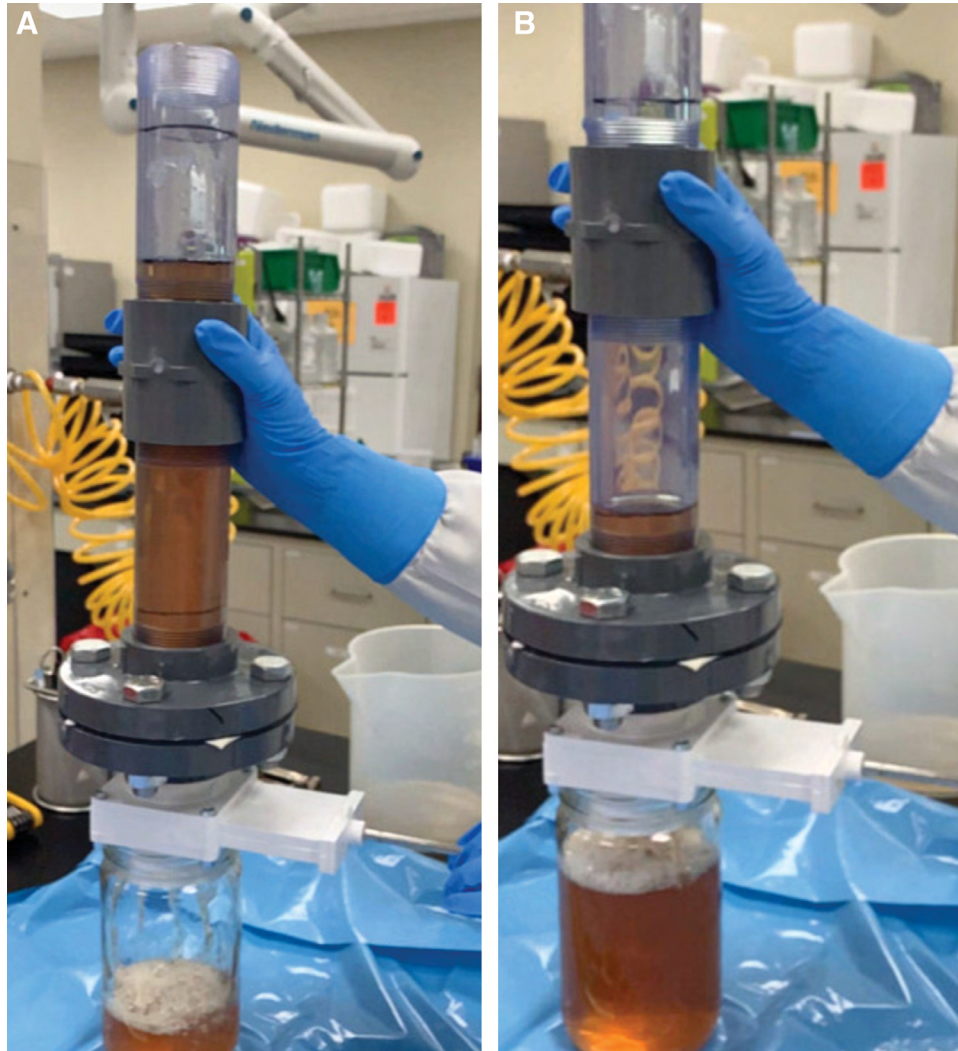


Fig. 5. Fluid egress testing device. The pipe was filled to the fill line (A) with FBS, and the time (in seconds) was recorded as the fluid level passed from the top container into the bottom container (B).

Perforation Pattern

In a 16 × 20cm graft, the area of a perforated surface is calculated as follows:

$$\text{Surface Area}_{\text{Perforated}} = (\text{area of top graft}) + (\# \text{ holes}) \times (\text{area of inside hole})$$

Perforation pattern #1 is calculated as follows:

$$\text{Surface Area}_{\text{Perforated}\#1} = 317.1018\text{cm}^2 + (41 \text{ holes}) (0.09424\text{cm}^2)$$

$$\text{Surface Area}_{\text{Perforated}\#1} = 320.966\text{cm}^2$$

$$\text{Original Graft Area} = (16 \text{ cm}) (20 \text{ cm}) = 320\text{cm}^2$$

$$\text{Increase in Surface Area from Perforation \#1} = \frac{(320.966 - 320)}{320} \times 100 = 0.3\%$$

Perforation pattern #2 is calculated as follows:

$$\text{Surface Area}_{\text{Perforated}\#2} = 314.34513\text{cm}^2 + (80) (0.09424\text{cm}^2)$$

$$\text{Surface Area}_{\text{Perforated}\#2} = 321.884\text{cm}^2$$

$$\text{Original Graft Area} = (16\text{cm}) (20\text{cm}) = 320\text{cm}^2$$

$$\text{Increase in Surface Area from Perforation \#2} = \frac{(321.884 - 320)}{320} \times 100 = 0.59\%$$

Therefore, perforation at either of these 2 densities yields less than a 1% increase in the total surface area of the ADM tissue.

DISCUSSION

Acellular dermal matrices have found routine use in implant-based breast reconstruction. Like any graft, for ADM to become revascularized, it must be in contact with a well-vascularized bed of tissue. Thus, it is generally accepted that creating holes in the ADM can facilitate

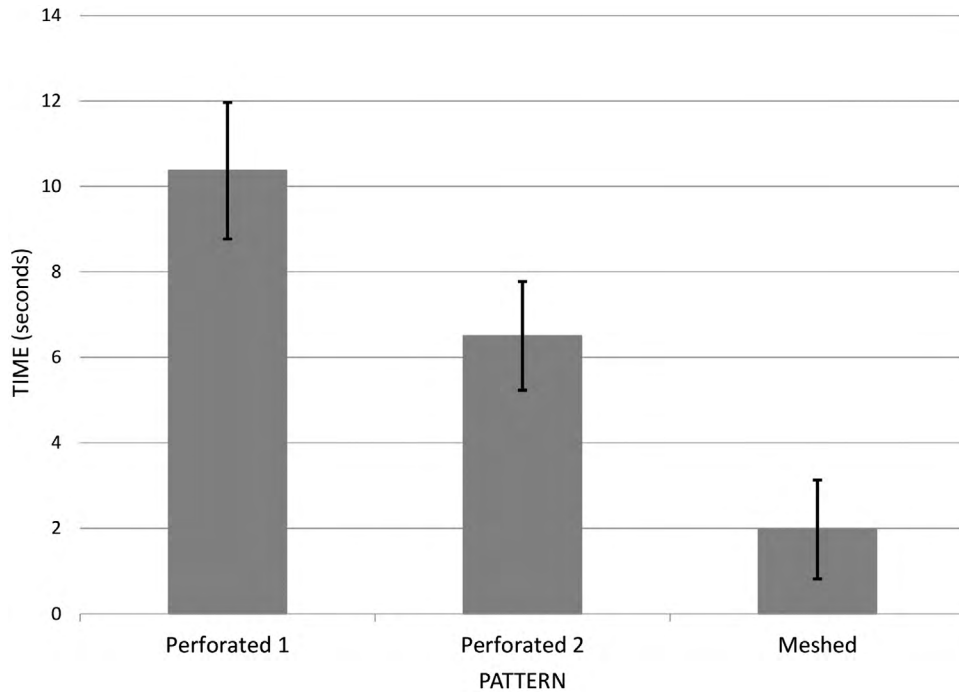


Fig. 6. Average draining times for meshed and perforated ADM (error bars indicate SD).

fluid egress across the membrane. This not only prevents fluid from separating the ADM off the recipient tissue, but also increases the surface area of contact with the recipient bed. However, many of the commercially available products have variable patterns of perforations. To our knowledge, our study is the first to directly compare clinically applicable properties between different ADM perforation patterns. By comparing a variety of perforation patterns, ranging from simple punch-shape perforations to a full 1:1 mesh pattern, we were able to demonstrate that meshing significantly increases egress of fluid across the membrane and surface area available to contact the recipient bed of tissue.

In a recent study, Lotan and colleagues compared meshed versus non-meshed biologic material in the setting of breast reconstruction.¹¹ They demonstrated reduced rates of postoperative seroma, hematoma, and infection, and decreased time to drain removal. Our dry laboratory data corroborate these clinical findings. For example, we found that the meshed ADM allowed for an almost 3-fold increase in the rate of egress of fluid across the material. This may explain the decreased seroma rates observed in the above study, as a configuration that prevents the sequestration of fluid may easily prevent clinically relevant

fluid collections. Furthermore, an increased surface area of contact, as demonstrated in our study, may also contribute to an accelerated rate of incorporation and vascularization of the material into the mastectomy pocket. This would clearly also contribute to decreased fluid production and resultant seroma occurrences.

Additionally, we routinely encounter the meshed ADM several weeks after expansion is complete and the permanent implant is being placed in the clinical setting (Fig. 7). This allows us to subjectively evaluate the degree of incorporation of the ADM we use. At these procedures, the meshed ADM is generally well-incorporated into the overlying mastectomy skin and underlying muscle tissue as

Table 1. Timing of Fluid Egress, SD, and Confidence Interval for Each Perforation Pattern

Pattern	Average Time (s)	SD (s)	95% Confidence Interval
Perforated 1	10.369	1.598	(9.189, 11.549)
Perforated 2	6.504	1.273	(5.324, 7.683)
Meshed	1.974	1.157	(0.795, 3.154)



Fig. 7. 1:1 meshed ADM covering an implant in vivo. Note that the implant is well covered with the ADM having no contour irregularities.

evidenced by the ingrowth of the patient's own tissue into the interstices of the mesh. It is also interesting to note that the mesh appears to expand the most over the highest projecting parts of the expander and remains minimally stretched over the flatter parts such as the posterior aspect that is against the chest wall. Future studies are in progress to determine a methodology to objectively measure the degree of incorporation of ADM meshing patterns in vivo and the resulting differences in complication rates.

In this study, we selected various perforation and mesh patterns that closely resemble those that are available on commercially available products that are commonly used for breast reconstruction. Our dry-laboratory data indicate that a 1:1 mesh pattern significantly increases both fluid egress across the material and surface area available for direct contact with the recipient bed of tissue. It is likely that an increased mesh ratio, such as 2:1 or 3:1, would further increase these measured outcomes. However, more aggressive mesh ratios produce larger open spaces that are devoid of matrix. Because the purpose of using ADM in breast reconstruction is to provide soft tissue augmentation to reinforce the otherwise thin, and often deficient, soft tissue coverage of the implant and its associated pocket, increasing the mesh ratio beyond the 1:1 ratio is not recommended.

Another very important property of any material that might be used for soft tissue augmentation in breast reconstruction is its ability to stretch with tissue expansion or when placed over a spherical implant. Although it is expected that meshing would improve the ability of any material to stretch over an irregular surface, it is not an endpoint evaluated here. Future studies aimed at assessing this property might add further evidence to determine the ideal biologic material for soft tissue augmentation in breast reconstruction.

CONCLUSIONS

This quantitative comparison revealed that meshing ADM tissue significantly improves fluid egress properties and substantially increases the surface area compared with ADM tissue perforated at levels (or beyond those)

typically available on the market. Meshing increases fluid flow out of the surgical site, enhances conformability, and increases the surface area of the graft.

Keith Sweitzer, MD

University of Rochester Medical Center
Rochester, NY

E-mail: keithsweitzer6@gmail.com

REFERENCES

1. Kim JYS, Mlodinow AS. What's new in acellular dermal matrix and soft-tissue support for prosthetic breast reconstruction. *Plast Reconstr Surg*. 2017;140(5S Advances in Breast Reconstruction):30S–43S.
2. Bertasi G, Cole W, Samsell B, et al. Biological incorporation of human acellular dermal matrix used in Achilles tendon repair. *Cell Tissue Bank*. 2017;18:403–411.
3. Nilsen TJ, Dasgupta A, Huang YC, et al. Do processing methods make a difference in acellular dermal matrix properties? *Aesthet Surg J*. 2016;36(suppl 2):S7–S22.
4. Garcia O Jr, Scott JR. Analysis of acellular dermal matrix integration and revascularization following tissue expander breast reconstruction in a clinically relevant large-animal model. *Plast Reconstr Surg*. 2013;131:741e–751e.
5. Sobti N, Ji E, Brown RL, et al. Evaluation of acellular dermal matrix efficacy in prosthesis-based breast reconstruction. *Plast Reconstr Surg*. 2018;141:541–549.
6. Spear SL, Seruya M, Clemens MW, et al. Acellular dermal matrix for the treatment and prevention of implant-associated breast deformities. *Plast Surg Nurs*. 2017;37:76–87.
7. Ganske I, Verma K, Rosen H, et al. Minimizing complications with the use of acellular dermal matrix for immediate implant-based breast reconstruction. *Ann Plast Surg*. 2013;71:464–470.
8. Lee KT, Mun GH. Updated evidence of acellular dermal matrix use for implant-based breast reconstruction: a meta-analysis. *Ann Surg Oncol*. 2016;23:600–610.
9. Israeli R. Complications of acellular dermal matrices in breast surgery. *Plast Reconstr Surg*. 2012;130(5 suppl 2):159S–172S.
10. Fosnot J, Kovach SJ III, Serletti JM. Acellular dermal matrix: general principles for the plastic surgeon. *Aesthet Surg J*. 2011;31(7 Suppl):5S–12S.
11. Maisel Lotan A, Ben Yehuda D, Allweis TM, et al. Comparative study of meshed and nonmeshed acellular dermal matrix in immediate breast reconstruction. *Plast Reconstr Surg*. 2019;144:1045–1053.